Sonochemical Method for the Preparation of Monodisperse Spherical and Rectangular Lead Selenide Nanoparticles

Jun-Jie Zhu,* Hui Wang, Shu Xu, and Hong-Yuan Chen

Department of Chemistry, Laboratory of Mesoscopic Science and State Key Laboratory of Coordination Chemistry, Nanjing University, Nanjing, 210093, People's Republic of China

Received June 27, 2001. In Final Form: January 3, 2002

Monodisperse lead selenide nanoparticles have been successfully prepared via a sonochemical route from an aqueous solution of lead acetate and sodium selenosulfate in the presence of complexing agents under ambient air. It was found that when trisodium citrate was used as the complexing agent, the product was spherical nanoparticles with an average size of ca. 8 nm. If potassium nitrilotriacetate was used, the product consisted of rectangles with an average size of ca. 25 nm. The products were characterized by powder X-ray diffraction, transmission electron microscopy, selected area electron diffraction, and X-ray photoelectron spectroscopy. A probable mechanism for the sonochemical formation of PbSe was proposed. Several factors that affected the nature and morphology of the products were also discussed such as the pH value, the complexing agents, and the intensity of the ultrasound irradiation.

Introduction

Nanocrystalline semiconductor particles have been the focus of scientific research in the past two decades because of their special properties such as a large surface-to-volume ratio, increased activity, special electronic properties, and unique optical properties as compared to those of the bulk materials.[1,2] Semiconductor selenides have attracted considerable attention due to their interesting properties and potential applications. They have been widely used as thermoelectric cooling materials, optical filters, optical recording materials, solar cells, superionic materials, and sensor and laser materials.[3−6] Conventional methods for the preparation of selenides include gas-phase reactions between the element or its compounds and gaseous H_2-Se,[7] solid-state reactions,[8] chemical bath deposition,[9] and pyrolysis of single source precursors.[10,11] Generally, all these methods have some limits. Finding a convenient, mild, and efficient method for the preparation of nanocrystalline selenides is still a challenge to synthetic chemists and materials scientists.

Ultrasound has become an important tool in chemistry in recent years. The sonochemical method has been used extensively to generate novel materials with unusual properties, since they form particles of a much smaller size and higher surface area than those reported by other methods.[12] The chemical effects of ultrasound arise from acoustic cavitation, that is, the formation, growth, and implosive collapse of bubbles in a liquid. The implosive collapse of the bubbles generates a localized hotspot through adiabatic compression or shock wave formation within the gas phase of the collapsing bubbles. When solutions are exposed to strong ultrasound irradiation, bubbles in the solution are implosively collapsed by acoustic fields, and high-temperature and high-pressure fields are produced at the centers of the bubbles. The temperature is estimated to be 5000 K, the pressure reaches over 1800 atm, and the cooling rate is in excess of 10^6 K/s when the bubbles implode,[13] which enables many chemical reactions to occur. These extreme conditions attained during bubble collapse have been exploited to prepare various materials including metals,[13−16] metal carbides,[17] metal oxides,[18−21] and metal chalcogenides.[22−25] The sonochemical method offers a very attractive method for the preparation of nanosized materials and has shown very rapid growth in its application to materials science due to its unique reaction effects.

PbSe is one kind of the most attractive selenides for a wide variety of applications in IR detectors, photographic plates, selective and photovoltaic absorbers, and so forth.[26] During the past two decades, PbSe has also been the object of an inquiry into nanosized effects. PbSe has been

* Corresponding author. E-mail: gxyz@nju.edu.cn. Fax: +86-25-3317761. Tel: +86-25-3594976.

(1) Henglein, A. *Chem. Rev.* **1989**, *89*, 1861.
(2) Agfeldt, A.; Gratzel, M. *Chem. Rev.* **1995**, *95*, 49.
(3) Mongellaz, F.; Fillot, A.; Griot, R.; De Lallee, J. *Proc. SPIE-Int. Soc. Opt. Eng.* **1994**, *156*, 2227.
(4) Wang, W. Z.; Geng, Y.; Yan, P.; Liu, F. Y.; Xie, Y.; Qian, Y. T. *J. Am. Chem. Soc.* **1999**, *121*, 4062.
(5) Lakshmikvmar, S. T.; Rastogi, A. C. *Sol. Energy Mater. Sol. Cells* **1994**, *32*, 7.
(6) Korzhuev, M. A. *Fiz. Khim. Obrab. Mater.* **1991**, *3*, 131.
(7) Metcalf, H. C.; Willams, J. E.; Caskata, J. F. *Modern Chemistry*; Holt, Reinhart, Winston: New York, 1982; p 54.
(8) Coustal, R. J. *J. Chim. Phys.* **1958**, *38*, 277.
(9) Lokhande, C. D.; Patil, P. S.; Tributsch, H; Ennaoui, A. *Sol. Energy Mater. Sol. Cells* **1998**, *55*, 379.
(10) Steigerwald, M. L.; Alivisatos, A. P.; Gibson, J. M. *J. Am. Chem. Soc.* **1988**, *110*, 3046.
(11) Ptatschek, V.; Schreder, B.; Herz, K. *J. Phys. Chem. B* **1997**, *101*, 8898.
(12) Suslick, K. S. *Ultrasound: Its Chemical, Physical and Biological Effects*; VCH: Weinhein, Germany, 1988.
(13) Suslick, K. S.; Choe, S. B.; Cichowlas, A. A.; Grinstaff, M. W. *Nature* **1991**, *353*, 414.
(14) Koltypin, Yu.; Katabi, G.; Prozorov, R.; Gedanken, A. *J. Non-Cryst. Solids* **1996**, *201*, 159.
(15) Nagata, Y.; Mizukoshi, Y.; Okitsu, K.; Maeda, Y. *Radiat. Res.* **1996**, *146*, 333.
(16) Okitsu, K.; Mizukoshi, Y.; Bandow, H.; Maeda, Y.; Yamamoto, T.; Nagata, Y. *Ultrason. Sonochem.* **1996**, *3*, 249.
(17) Hyeon, T.; Fang, M.; Suslick, K. S. *J. Am. Chem. Soc.* **1996**, *118*, 5492.
(18) Cao, X.; Koltypin, Yu.; Katabi, G.; Felner, I.; Gedanken, A. *J. Mater. Res.* **1997**, *12*, 405.
(19) Arul Dhas, N.; Gedanken, A. *J. Phys. Chem. B* **1997**, *101*, 9495.
(20) Kumar, R. V.; Diamant, Y.; Gedanken, A. *Chem. Mater.* **2000**, *12*, 2301.
(21) Patra, A.; Sominska, E.; Ramesh, S.; Koltypin, Yu.; Zhong, Z.; Minti, H.; Reisfeld, R.; Gedanken, A. *J. Phys. Chem. B* **1999**, *103*, 3361.
(22) Zhu, J. J.; Koltypin, Yu.; Gedanken, A. *Chem. Mater.* **2000**, *12*, 73.
(23) Li, B.; Xie, Y.; Huang, J. X.; Liu, Y.; Qian, Y. T. *Chem. Mater.* **2000**, *12*, 2614.
(24) Mdleleni, M. M.; Hyeon, T.; Suslick, K. S. *J. Am. Chem. Soc.* **1998**, *120*, 6189.
(25) Wang, G. Z.; Wang, Y. W.; Chen, W.; Liang, C. H.; Li, G. H.; Zahang, L. D. *Mater. Lett.* **2001**, *48*, 269.

10.1021/la010988q CCC: $22.00
Published on Web 03/20/2002

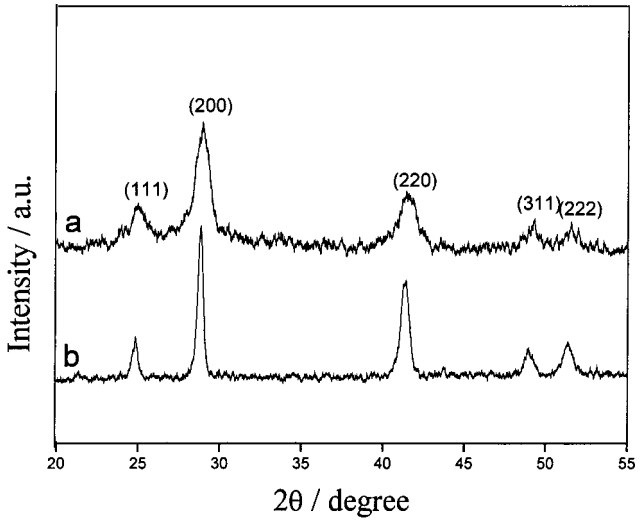

Figure 1. Powder XRD patterns of (a) sample A and (b) sample B.

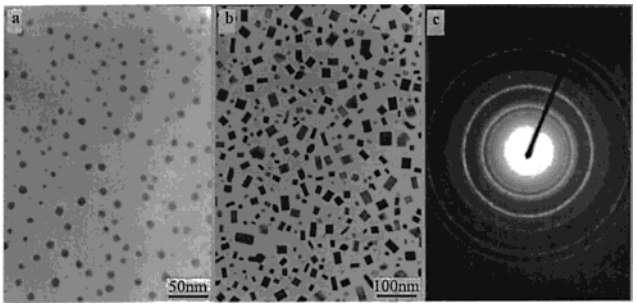

Figure 2. TEM images of (a) sample A and (b) sample B and (c) ED picture of sample A.

Table 1. The Results of Characterizations

complexing agent used		dimensions from XRD (nm)	TEM morphology	TEM particle size (nm)	element ratio of Pb/Se from XPS
sample A	TSC	8	spherical	5−10	6:4
sample B	NTA	25	rectangular	20 × 27	6:4

prepared by various methods such as chemical bath deposition,[27,28] molecular beam epitaxy,[29] vacuum deposition,[30] electrodeposition,[31,32] the pulse sonoelectrochemical method,[33] the photochemical method,[34] microwave assisted heating,[35] and the successive ionic layer adsorption and reaction technique.[36]

Sonochemical synthesis of PbSe nanoparticles was first reported by Qian et al.[37,38] They chose ethylenediamine as the solvent and used a commercial ultrasound cleaner as the ultrasound irradiation source. The products were agglomerated spherical particles with average sizes of 30 and 160 nm. Kerner et al. also managed to prepare rectangular PbSe nanoparticles via a sonochemical polyol reduction route.[39] However, they chose ethylene glycol as the solvent which restrained the development of a bubble to its full size due to its high viscosity. In this respect, ethylene glycol is not a favorable solvent for sonochemistry.

Herein, lead selenide nanoparticles have been successfully prepared via a sonochemical route from an aqueous solution of lead acetate and sodium selenosulfate in the presence of complexing agents under ambient air. We managed to prepare monodisperse PbSe nanoparticles with different morphologies by using different complexing agents. It is found to be a convenient and efficient route to produce monodisperse PbSe nanoparticles with controllable morphologies in only one step.

Experimental Section

All the reagents used were of analytical purity and used without further purification. $Pb(CH_3COO)_2 \cdot 3H_2O$, trisodium citrate (TSC), and Na_2SO_3 were purchased from Shanghai Second Chemical Reagent Factory (China). Absolute ethanol, acetone, and KOH were purchased from Nanjing Chemical Reagent Factory (China). Se and potassium nitrilotriacetate (NTA) were purchased from Aldrich Co. Distilled water was used in our experiments.

In a typical procedure, an aqueous solution of $Pb(CH_3COO)_2$ in the presence of complexing agents was mixed with 0.2 M Na_2SeSO_3 solution in a 150 mL round-bottom flask to give a final concentration of 20 mM $Pb(CH_3COO)_2$, 40 mM complexating agents, and 20 mM Na_2SeSO_3. The pH was adjusted to 10 by KOH, and the total volume of the solution was 100 mL. Na_2SeSO_3 solution (0.2 M) was prepared by stirring 0.2 M Se and 0.5 M Na_2SO_3 at ca. 70 °C for 24 h. The complexing agents used in the experiments were TSC and NTA, and the corresponding products were designated as sample A and sample B, respectively. Then the mixture solution was exposed to high-intensity ultrasound irradiation under ambient air for 30 min. Ultrasound irradiation was accomplished with a high-intensity ultrasonic probe (Xinzhi. Co., China, JY92-2D, 0.6 cm diameter; Ti-horn, 20 kHz, 60 W/cm^2) immersed directly in the reaction solution. Then a great amount of black precipitates occurred. After the mixture was cooled to room temperature, the precipitates were centrifuged, washed by distilled water, absolute ethanol, and acetone in sequence, and dried in air. The final products were collected for characterizations. The products have been characterized by X-ray powder diffraction (XRD), transmission electron microscopy (TEM), selected area electron diffraction (ED), and X-ray photoelectron spectroscopy (XPS).

The XRD analysis was performed by a Shimadzu XD-3A X-ray diffractometer at a scanning rate of 4°/min in the 2θ range from 15° to 60°, with graphite monochromatized Cu Kα radiation ($\lambda = 0.15418$ nm). Transmission electron micrographs and electron diffraction patterns were obtained by employing a JEOL JEM-200CX transmission electron microscope, using an accelerating voltage of 200 kV. The surface of the products was detected by X-ray photoelectron spectra recorded on an ESCALAB MK II X-ray photoelectron spectrometer, using nonmonochromatized Mg Kα X-rays as the excitation source. A Ruili 1200 photospectrometer (Peking Analytical Instrument Co.) was used to record the UV−visible absorption spectra of the as-prepared particles.

Results and Discussion

To study the nature and morphology of the products, characterization techniques including powder XRD, TEM,

(26) Mulik, R. N.; Rotti, C. B.; More, B. M.; Sutrave, D. S.; Shahane, G. S.; Garadkar, K. M.; Deshmukh, L. P.; Hankare, P. P. *Indian J. Pure Appl. Phys.* **1996**, *34*, 903.
(27) Gorer, S.; Albu-Yaron, A.; Hodes, G. *Chem. Mater.* **1995**, *7*, 1243.
(28) Gorer, S.; Albu-Yaron, A.; Hodes, G. *J. Phys. Chem.* **1995**, *99*, 16442.
(29) Zogg, H.; Maissen, C.; Masek, J.; Hoshion, T.; Blunier, S.; Tiwari, A. N. *Semicond. Sci. Technol.* **1991**, *6*, C36.
(30) Das, D. V.; Bhat, K. S. *J. Mater. Sci.* **1990**, *1*, 169.
(31) Saloniemi, H.; Kanniainen, T.; Ritala, M.; Leskela, M.; Lappalainen, R. *J. Mater. Chem.* **1998**, *8*, 651.
(32) Molin, A. N.; Dikusar, A. I. *Thin Solid Films* **1995**, *265*, 3.
(33) Zhu, J. J.; Aruna, S. T.; Koltypin, Yu.; Gedanken, A. *Chem. Mater.* **2000**, *12*, 143.
(34) Zhu, J. J.; Liao, X. H.; Wang, J.; Chen, H. Y. *Mater. Res. Bull.* **2001**, *36*, 1169.
(35) Zhu, J. J.; Palchik, O.; Chen, S. G.; Gedanken, A. *J. Phys. Chem. B* **2000**, *104*, 7344.
(36) Kanniainen, T.; Lindroos, S.; Ihanus, J.; Leskela, M. *J. Mater. Chem.* **1996**, *6*, 983.
(37) Zhan, J. H.; Yang, X. G.; Wang, D. W.; Xie, Y.; Qian, Y. T. *Inorg. Chem. Commun.* **1999**, *2*, 447.
(38) Li, B.; Xie, Y.; Huang, J.; Qian, Y. T. *Ultrason. Sonochem.* **1999**, *6*, 217.
(39) Kerner, R.; Palchik, O.; Gedanken, A. *Chem. Mater.* **2001**, *13*, 1413.

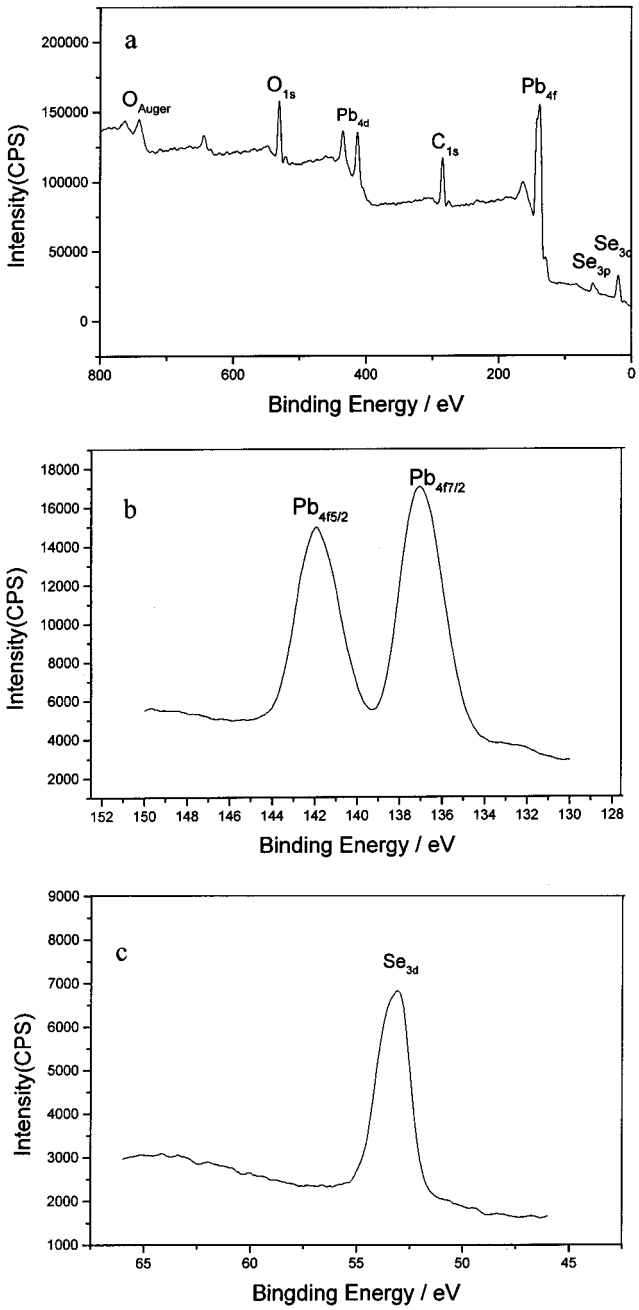

Figure 3. (a) Wide XPS picture of sample A, (b) high-resolution XPS spectrum of Pb(4f), and (c) high-resolution XPS spectrum of Se(3d).

ED, and XPS were employed. The results of the characterizations are listed in Table 1.

XRD Study. The powder XRD patterns of sample A and sample B are shown in Figure 1. The diffraction peaks correspond to the (111), (200), (220), (311), and (222) planes, which can be indexed to the pure clausthalite phase for PbSe. No peak of any other phase is detected. The intensities and positions of the peaks are in perfect agreement with the literature values.[40] Both products have a rock-salt (NaCl) structure. The broadening of the peaks indicates that the crystallite size is small. The average particle sizes of sample A and sample B are calculated to be 8 and 25 nm, respectively, according to the Debye–Scherrer equation.[41]

(40) JCPDS Card File, No. 6-354.

(41) *X-ray Diffraction Procedures*; Klug, H., Alexander, L., Eds.; Wiley: New York, 1962; p 125.

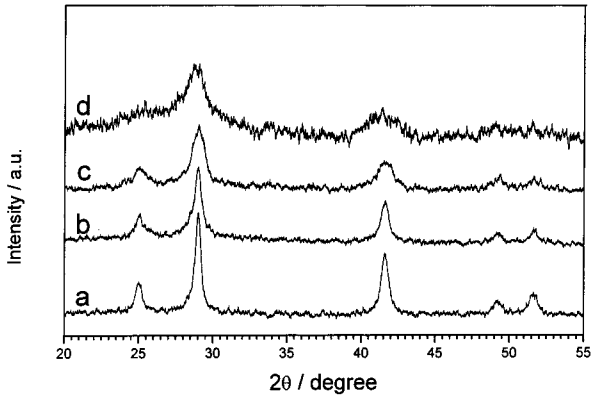

Figure 4. XRD patterns of PbSe nanoparticles prepared in different amounts of TSC: (a) 160 mM TSC; (b) 80 mM TSC; (c) 40 mM TSC; (d) PbSe nanoparticles prepared by using a sonic intensity of 20 W/cm^2.

TEM and ED Measurements. TEM images of sample A and sample B are presented in parts a and b of Figure 2. Figure 2a shows that sample A consists of monodisperse spherical nanoparticles. The diameters of the particles are in the range of 5−10 nm, which is in accordance with the result calculated from the XRD pattern. In Figure 2b, monodisperse rectangular particles are observed. Some of these particles are partially elongated. The mean dimensions of these species are calculated from the transmission electron micrograph by averaging over a few hundred species. The average length and width are calculated to be 27 and 20 nm, respectively. This result also agrees with the Scherrer calculated size.

The crystallinity and crystallography of the products are proven by selected area electron diffraction. Figure 2c shows the electron diffraction pattern of sample A. It shows that this product is polycrystalline and the diffraction rings match the XRD peaks very well. A similar result is obtained on the ED pattern of sample B.

XPS Analysis. The products were characterized by XPS for evaluation of their composition and purity. The wide-scan X-ray photoelectron spectrum of sample A is shown in Figure 3a. The binding energies obtained in the XPS analysis are standardized for specimen charging using C(1s) as the reference at 284.6 eV. No peaks of other elements except C, O, Pb, and Se were observed in the picture, indicating the high purity of this product.

Parts b and c of Figure 3 show the high-resolution XPS spectra of Pb(4f) and Se(3d), respectively. The two strong peaks taken for the Pb region at 136.9 and 142.0 eV are assigned to the Pb(4f) binding energy. The peak measured in the Se energy region detected at 53.1 eV is attributed to the Se(3d) transition. The atomic ratio of Pb/Se calculated on the basis of the Pb(4f) and Se(3d) spectra is approximately 6:4, which shows that the surface of the product is rich in lead. Similar results are obtained from the XPS measurements of sample B.

The mechanism of the sonochemical formation of PbSe nanoparticles is probably related to the radical species generated from water molecules by the absorption of the ultrasound energy. An ultrasound wave that is intense enough to produce cavitation can drive chemical reactions such as oxidation, reduction, dissolution, and decomposition.[12,42] Other reactions driven by high-intensity ultrasound irradiation such as promotion of polymerization have also been reported. It has been known that during an aqueous sonochemical process, the elevated temper-

(42) Suslick, K. S.; Hammerton, D. A.; Cline, R. E. *J. Am. Chem. Soc.* 1986, *108*, 5641.

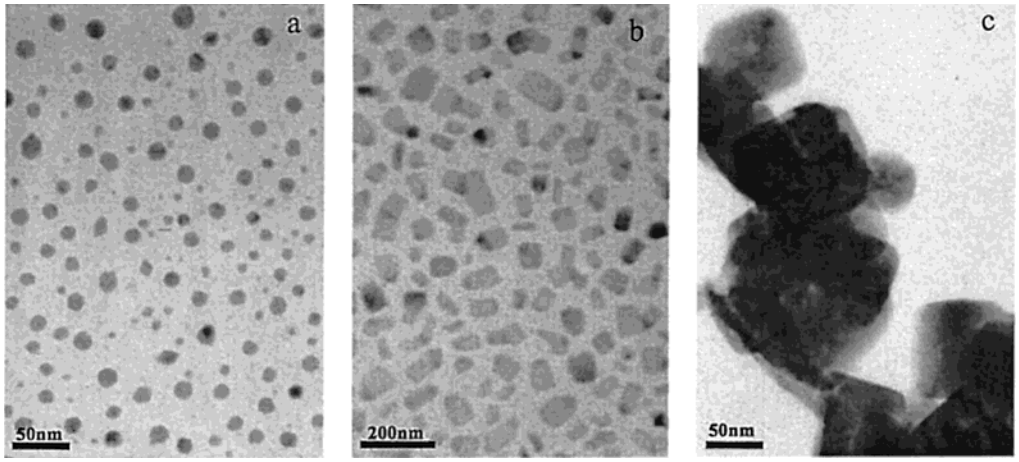

Figure 5. TEM images of the PbSe nanoparticles (a) prepared in the presence of 80 mM TSC, (b) prepared in the presence of 160 mM TSC, and (c) prepared in the presence of a high concentration of KOH (pH = 14).

atures and pressures inside the collapsing bubbles cause water to vaporize and further pyrolyze into $H^{\bullet}$ and $OH^{\bullet}$ radicals. The probable reaction process for the sonochemical formation of PbSe nanoparticles in aqueous solution can be summarized as follows:

$$Pb(TSC)_2^{4-} \rightleftharpoons Pb^{2+} + 2TSC^{3-} \quad \text{or}$$
$$Pb(NTA)_2^{4-} \rightleftharpoons Pb^{2+} + 2NTA^{3-} \quad (1)$$

$$H_2O \rightarrow H^{\bullet} + OH^{\bullet} \quad (2)$$

$$2H^{\bullet} + SeSO_3^{2-} \rightarrow Se^{2-} + 2H^{+} + SO_3^{2-} \quad (3)$$

$$Pb^{2+} + Se^{2-} \rightarrow PbSe \quad (4)$$

$$n\text{PbSe} \rightarrow (\text{PbSe})_n \quad (5)$$

Initially, the complexing actions between Pb^{2+} and TSC or NTA lead to the formation of Pb−TSC or Pb−NTA complexes. Reaction 2 represents the formation of primary radicals by the ultrasound-initiated dissociation of water within the collapsing gas bubbles. Reactions 3−5 represent the main steps leading to the formation of PbSe nanoparticles. The in situ generated $H^{\bullet}$ is a highly reducing radical and can react with $SeSO_3^{2-}$ ions rapidly via reaction 3 to form Se^{2-} ions. Then Se^{2-} ions combine with Pb^{2+} ions which are released from the Pb−TSC or Pb−NTA complexes to yield PbSe nuclei. These freshly formed nuclei in the solution are unstable and have the ability to grow into larger PbSe particles.

The complexing agents play an important role in the formation of PbSe nanoparticles. The complexing agents can reduce the concentration of free Pb^{2+} in the solution and affect the reaction rate. The complexing strength of NTA with Pb^{2+} is stronger than that of TSC. So when TSC is used as the complexing agent, the nucleation rate is faster. When TSC was used, we found that after sonication for 15 min, the transparent solution became dark brown and turbid, indicating the formation of PbSe nuclei. After 30 min, the reaction was completed, and a black precipitate was obtained. In the case of NTA, the nucleation rate became slower, and it took 20 min for the PbSe nuclei to form. As a result, the size of the product prepared using TSC as the complexing agent is smaller than that prepared in the presence of NTA. Furthermore, the complexing agents used in our experiments also affect the morphology of the as-prepared PbSe nanoparticles. When TSC was used, the as-prepared nanoparticles were spherical in shape. In the case of NTA, the particles obtained were partially elongated rectangles. The amount of the complexing agent also has an influence on the particle size of the products. Figure 4a−c shows the XRD patterns of the PbSe nanoparticles prepared in the presence of different amounts of TSC. We found that the as-prepared PbSe nanoparticles became larger with the increase of the TSC/Pb ratio. If the concentration of TSC was changed to 80 mM and all the other preparation conditions remained unchanged, the particle size of the product increased to 10−15 nm, as we calculated from the XRD pattern and observed in its TEM image (Figure 5a). When the concentration of TSC increased to 160 mM, the size of the product became even larger, and its morphology changed to be rectangular-like (Figure 5b). When the ratio of TSC/Pb increases, the concentration of free Pb^{2+} ions in the solution decreases. As a result, the nucleation rate of PbSe becomes slower, which is favorable for the nuclei to grow into larger grains. However, in the case of NTA, the effect of complexant amount on the particle size is not as conspicuous as that of TSC. When the Pb/NTA ratio was in the range of 1:1 to 1:4, the average particle sizes of the products remained almost the same. In these cases, maybe the amount of NTA does not have a conspicuous influence on the nucleation rate of PbSe.

The pH of the reaction is also one of the most important factors. A pH range of 9−11 is optimal. Some impurities such as elemental Se were obtained at pHs lower than 7. The reason may be that the oxidation and reduction potentials of Se are pH dependent and free Se is released when the pH is lower than 7. If the pH value is higher than 13, another complex, $Pb(OH)_x^{2-x}$, was formed due to the high concentration of OH^- and the stronger complexing strength between Pb^{2+} and OH^-. In this case, the as-prepared particles become much larger (ca. 100 nm) and are in an aggregated state as we can see on the transmission electron micrograph (Figure 5c).

We have also carried out experiments to investigate the effects of the ultrasonic intensity. We found that it took a longer period of time for the PbSe nuclei to form if the stock solution is exposed to ultrasound irradiation with a lower intensity. When we used a sonic intensity of 20 W/cm^2 to carry out the experiments and all the other preparation conditions were the same as those of sample A, the PbSe nuclei began to form after 90 min, and it took 3 h for the reaction to be completed. The average size of this product was estimated to be smaller than 5 nm from the XRD pattern (Figure 4d). On the transmission electron micrograph (Figure 6), we observed that this sample

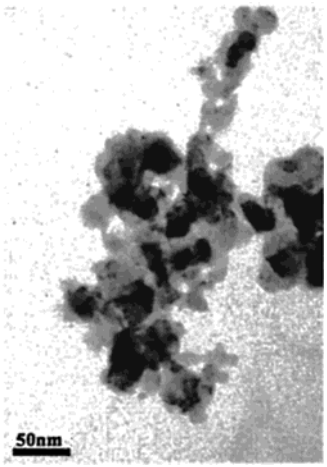

Figure 6. TEM image of the PbSe nanoparticles prepared in the presence of 20 W/cm^2 ultrasound irradiation.

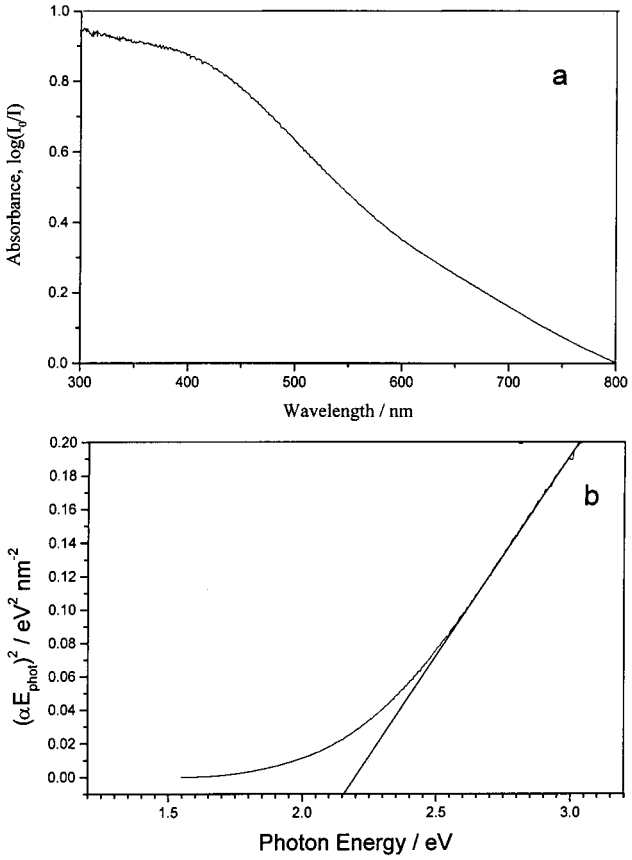

Figure 7. (a) The UV−vis absorbance spectra of PbSe nanoparticles (in EtOH suspension) prepared using 20 W/cm^2 sonic intensity; (b) plots of $(\alpha E_{phot})^2$ vs E_{phot} for direct transitions.

consisted of nanoparticles with diameters ranging from 2 to 5 nm in an aggregated state. These particles were held together by an irregular network. The Gibbs free energy of the surface of small-sized nanoparticles is usually very high due to the large surface-to-volume ratio. These small particles have the tendency to aggregate together to decrease the Gibbs free energy of the surface and make the surface state stable. In most cases, the nanoparticles aggregate together more easily with the decrease in size. Though monodisperse PbSe nanoparticles cannot be obtained when 20 W/cm^2 is used, we still pay much attention to this sample due to its small size and the conspicuous quantum size effects it presents. For a crystallite size less than the Bohr diameter (ca. 80 nm for PbSe), an increase in the effective band gap due to size quantization should begin to be apparent. We have carried out the UV−visible absorption spectrum of this product in order to resolve the excitonic or interband transitions of PbSe nanoparticles. The UV−visible absorption spectrum of this sample dispersed in ethanol solution (the concentration is 0.202 mg/mL) is shown in Figure 7a. An estimate of the optical band gap is obtained using the following equation for a semiconductor:

$$\alpha(\nu) = A(h\nu/2 - Eg)^{m/2}$$

where A is a constant, α is the absorption coefficient, and m equals 1 for a direct transition. The energy intercept of a plot of $(\alpha E_{phot})^2$ versus E_{phot} yields Eg for a direct transition (Figure 7b).[46] The band gap of this sample is calculated to be 2.15 eV from the UV−visible absorption spectrum, which is much larger than the reported value for bulk PbSe (Eg = 0.29 eV).[47] Light absorption leads to an electron in the conduction band and a positive hole in the valence band. In small particles, they are confined to potential wells of small lateral dimension and the energy difference between the position of the conduction band and a free electron, which leads to a quantization of their energy levels. The phenomena arise when the size of the particles becomes comparable to the de Broglie wavelength of a charge carrier. The increase in the band gap of the as-prepared PbSe nanoparticles is indicative of size quantization effects.[48] Hodes reported the quantum effects of lead selenide film. Different sizes of PbSe have different band gaps, which vary from 0.55 to 1.55 eV.[28] Gedanken and co-workers also reported the band gap of 12 nm PbSe nanoparticles prepared by the pulse sonoelectrochemical method to be 1.1 eV.[33] Herein, the as-prepared PbSe nanoparticles are smaller than those reported, so the band gap becomes even larger.

Conclusion

In summary, monodisperse spherical and rectangular lead selenide nanoparticles can be successfully prepared via a sonochemical route from an aqueous solution of lead acetate and sodium selenosulfate in the presence of complexing agents under ambient air. The morphologies and sizes of the particles can be obtained by controlling experimental conditions. Further studies may extend this method for the preparation of other nanocrystalline selenide semiconductors.

Acknowledgment. This work is supported by the National Natural Science Foundation of China (No. 50072006 and No. 20075010) and the Jiangsu Science and Technology Foundation (BG 2001039). The authors also thank Ms. Xiaoning Zhao and Ms. Xiaoshu Wang, Modern Analytic Center of Nanjing University, for extending their facilities to us.

LA010988Q

(43) Lauterborn, W.; Vogel, A. *Annu. Rev. Fluid Mech.* **1984**, *16*, 223.
(44) Ramech, S.; Koltypin, Yu.; Gedanken, A. *J. Mater. Res.* **1997**, *12*, 3271.
(45) Chen, W.; Wang, Z.; Lin, Z.; Lin, L. *J. Appl. Phys.* **1997**, *82*, 3111.
(46) Tsunekawa, S.; Fukuda, T.; Kasuya, A. *J. Appl. Phys.* **2000**, *87*, 1319.
(47) Streltov, E. A.; Osipovich, N. P.; Ivashkevich, L. S.; Lyakhov, A. S.; Sviridov, V. V. *Electrochim. Acta* **1998**, *43*, 869.
(48) Yang, J, P.; Meldrum, F. C.; Fendler, J. H. *J. Phys. Chem.* **1995**, *99*, 5500.